Available online at www.sciencedirect.com
ScienceDirect
C. R. Chimie 12 (2009) 692–698
COMPTES RENDUS CHIMIE

Full paper / Mémoire

Preparation of new oxidic precursors based on heteropolyanions for efficient hydrocracking catalysts

Karima Ben Tayeb [a], Carole Lamonier [a,*], Christine Lancelot [a], Michel Fournier [a], Edmond Payen [a], F. Bertoncini [b], A. Bonduelle [b]

[a] *Unité de catalyse et chimie du solide, UMR 8181, Université des sciences et technologies de Lille, bâtiment C3, 59655 Villeneuve d'Ascq, France*
[b] *Institut français du pétrole, rond-point de l'échangeur de Solaize, BP 3, 69360 Solaize, France*

Received 7 May 2008; accepted after revision 8 October 2008
Available online 16 March 2009

Abstract

Hydrocracking catalysts are bifunctional, associating a hydro–deshydrogenating function with an acidic one. If gas oil is the required product, NiW/silica–alumina is the most appropriate catalyst. It is obtained through the sulfidation of an oxidic precursor that is prepared by incipient wetness impregnation of the support by ammonium metatungstate and nickel nitrate solution. After impregnation the solid is matured, dried and calcined. We focused here on the use of tungsten heteropolyanions as $NiW_6O_{24}H_6^{4-}$ (Anderson-type) or $SiW_{12}O_{40}^{4-}$, $PW_{12}O_{40}^{3-}$ and $PW_{11}NiO_{40}H^{6-}$ (Keggin-type) to prepare the impregnating solution. Nickel salts of the Keggin heteropolytungstate were synthesized in order to associate W and Ni in the same entity. The first catalytic results in toluene hydrogenation showed the efficiency of the Keggin-type HPA NiW/ASA catalysts. ***To cite this article: K. Ben Tayeb et al., C. R. Chimie 12 (2009).***

Résumé

Les catalyseurs d'hydrocraquage sont bi-fonctionnels et allient une fonction acide et une fonction hydro-déshydrogénante. Les formulations les plus performantes qui conduisent à l'obtention de gasoils et kérosène sont de type NiW/silice–alumine. Le catalyseur est obtenu après sulfuration du précurseur oxyde. Ce dernier est lui-même préparé par imprégnation à sec du support par une solution de métatungstate d'ammonium et de nitrate de nickel, l'imprégnation étant suivie des étapes de maturation, séchage et calcination. Dans ce travail, nous cherchons à modifier la solution d'imprégnation en utilisant des précurseurs hétéropolyanioniques de type Anderson, tel $NiW_6O_{24}H_6^{4-}$ ou de type Keggin tels $SiW_{12}O_{40}^{4-}$, $PW_{12}O_{40}^{3-}$ et $PW_{11}NiO_{40}H^{6-}$, ces derniers étant sous forme de sels de nickel, de manière à associer dès la première étape de préparation l'espèce active W et son promoteur. Les premiers résultats dans la réaction test d'hydrogénation du toluène montrent que ces nouveaux catalyseurs sont efficaces en hydrocraquage. ***Pour citer cet article : K. Ben Tayeb et al., C. R. Chimie 12 (2009).***

Keywords: Hydrocracking; Heteropolytungstate; NiW catalyst; Raman; TEM; Toluene hydrogenation

Mots-clés : Hydrocraquage ; Hétéropolytungstate ; Catalyseur NiW ; Raman ; Microscopie électronique en transmission ; Hydrogénation du toluène

* Corresponding author.
E-mail address: carole.lamonier@univ-lille1.fr (C. Lamonier).

1631-0748/$ - see front matter
doi:10.1016/j.crci.2008.10.020

1. Introduction

The ever increasing demand for lighter engine fuel and the higher price of light crude oil has stimulated the petroleum refining industry into looking for the possibility of processing heavy fractions as well as cheaper heavy crude oil. In this context, hydrocracking process is of a major interest for the refiners. Hydrocracking catalysts are bifunctional associating a hydro–deshydrogenating function with an acidic one. The cracking activity is mainly controlled by the support. For supported catalysts, various supports as zeolithe [1], MCM [2] or ASA (amorphous silica alumina) [3,4] supported catalysts have been reported in the literature and among these supports, ASA possesses a moderate acidity which allows one to obtain an optimal gas oil yield. Since the feeds to be treated contain significant amounts of sulfur and nitrogen, the catalysts must resist poisoning by hydrogen sulphide and ammonia. The hydro–deshydrogenation function is then provided by mixed sulfides of W and Ni and the active phase consists in well-dispersed WS_2 nanocrystallites decorated with Ni atoms. This active phase is obtained through the sulphidation of an oxide precursor prepared by incipient wetness impregnation of ASA with an aqueous solution containing the elements to be deposited. To improve these catalysts, this work focuses on the interest of new starting materials for the preparation of the impregnating solutions, instead of ammonium metatungstate and nickel nitrate salts. Different heteropolytungstates, with Anderson, Keggin or its derived lacunary based structures have been prepared and characterized to be used as starting materials for the oxide precursors preparation. In particular, heteropolyanion (HPA) nickel salts have been prepared and impregnated on an ASA support to provide catalysts with varying Ni/W ratio, the WO_3 content being maintained at 12 wt%. All the HPA based catalysts were fully characterized in order to monitor the structure of oxide precursors as well as the dispersion of the active elements, at each step of preparation. Finally, hydrogenation activity of HPA based catalysts was also compared to the conventional preparation.

2. Experimental

2.1. Preparation of the Anderson HPA: $NiW_6O_{24}H_6^{4-}$

The Anderson ammonium salt $(NH_4)_4NiW_6O_{24}H_6$ was obtained according to literature data by precipitation from an aqueous solution of sodium tungstate, nickel sulfate and ammonium chloride at pH = 6 [5]. The recrystallization allows one to purify this ammonium salt. The Ni/W ratio (1/6) was checked by chemical analysis.

2.2. Preparation of the Keggin-type HPA nickel salts

The starting materials were the well-known pure heteropolyacids $H_3PW_{12}O_{40}$ and $H_4SiW_{12}O_{40}$ prepared according to the literature data [6,7]. The first step was the preparation of the barium salts in solution by ionic exchange of the acidic protons by barium cations. The nickel salts of the Keggin HPA $PW_{12}O_{40}^{3-}$ and of its derived lacunary HPA $PW_{11}O_{39}^{7-}$ (obtained by removing one WO_6 octahedron) were then obtained by a successive ionic exchange between barium and nickel cations.

The exchanges proceeded according to the following equations for the Keggin compound:

$$(3H^+, PW_{12}O_{40}^{3-}) + (1.5Ba^{2+}, 3OH^-) \rightarrow (1.5Ba^{2+}, PW_{12}O_{40}^{3-}) + 3H_2O$$

$$(1.5Ba^{2+}, PW_{12}O_{40}^{3-}) + 1.5(Ni^{2+} + SO_4^{2-}) \rightarrow (1.5Ni^{2+}, PW_{12}O_{40}^{3-}) + 1.5BaSO_4$$

The reactants were introduced into stoichiometric quantities and stirred vigorously at room temperature. The solution of the nickel salt was then filtered to eliminate the $BaSO_4$ white precipitate. Then the remaining solution was evaporated at room temperature to obtain $Ni_{3/2}PW_{12}O_{40}$ solid. $SiW_{12}O_{40}^{4-}$ nickel salt was synthesized by the same procedure as that for $PW_{12}O_{40}^{3-}$ nickel salt.

The nickel salt of the lacunary HPA $PW_{11}O_{39}^{7-}$ was also obtained following the same preparation procedure. The formation of the lacunary specie was due to the addition of 3.5 equivalent of barium hydroxide (instead 1.5). Indeed the pH of the solution raised to 3 and the more stable HPA specie was $PW_{11}O_{39}^{7-}$. This procedure is shown in Fig. 1.

The impregnating solutions were directly prepared, containing only Ni ions and the corresponding HPA. $BaSO_4$ was eliminated by filtration of the precipitate. The bulk compounds were afterwards obtained by evaporation.

2.3. Preparation of catalysts

Catalysts were prepared by incipient wetness impregnation of ASA support with Keggin HPA based solutions. Unfortunately the solubility of the ammonium

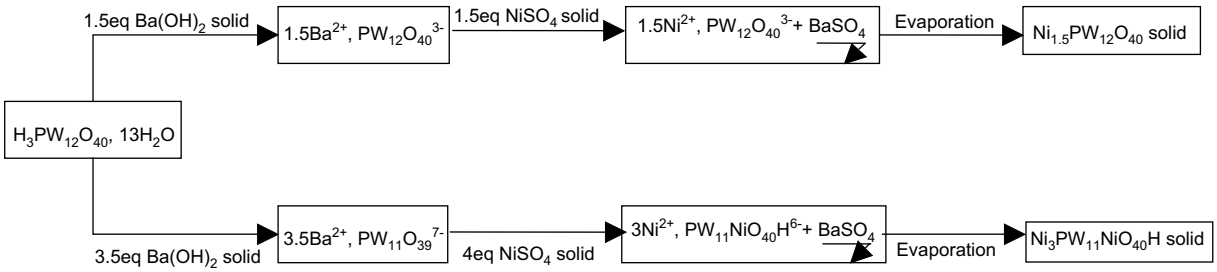

Fig. 1. Synthesis scheme for the preparation of the nickel salts of Keggin based heteropolyanions.

Anderson compound is too low to prepare catalyst with a suitable tungsten loading. No further study was then performed on this solid. Reference NiW solids having the same metal loadings were also prepared for comparison purposes by using the conventional impregnating solutions of ammonium metatungstate $(NH_4)_6H_2W_{12}O_{40}$ and nickel nitrate $Ni(NO_3)_2$. The solids were dried overnight at 100 °C and then calcined at 500 °C under oxygen. Oxide precursors were then sulfided in a glass vial at atmospheric pressure under a H_2S/H_2 mixture with a $p(H_2S)/p(H_2)$ ratio about 0.17 and a gas flow of 2 L/h/g of catalyst. The samples were heated under the sulfiding mixture at a rate of 5 °C/min up to 350 °C and maintained at this temperature for 2 h. They were then cooled down to room temperature under the reactive mixture.

Table 1 lists the different nickel salts, the corresponding Ni/W ratio – which was checked by chemical analysis – nomenclature of new materials based and reference catalysts. The quantity of WO_3 loading was chosen at 12 wt% because it is the maximum loading obtained for the lowest soluble Keggin HPA nickel salt.

2.4. Characterization techniques

FT-IR: Spectra were recorded using a Nicolet 510 Fourier Transform IR spectrometer. The samples were analyzed in the 200–4000 cm^{-1} spectral range using the KBr pellet technique with 1 wt% of the sample in KBr.

Raman: The Raman spectra of the samples, maintained at room temperature, were recorded using a Raman microprobe (Infinity from Jobin-Yvon), equipped with a photodiode array detector. The exciting light source was the 532 nm line of a Ar YAG laser and the wavenumber accuracy was 2 cm^{-1}. Due to the intense lines of ASA supports, only the 800–1200 spectral range characteristic of the W–O stretching mode is presented here.

TEM: Transmission electron microscopy studies were performed on a TECNAI electron microscope operating at an accelerating voltage of 200 kV. The sample was dispersed in ethanol and then deposited on carbon films supported on copper grids.

Table 1
Description of the catalysts prepared using the new starting materials or conventional impregnating solutions.

Catalysts nomenclature	Precursor	Ni/W	WO_3 loading (wt%)
A	$Ni_{3/2}PW_{12}O_{40}$	0.125	12
B	$Ni_2SiW_{12}O_{40}$	0.17	12
C	$Ni_3PW_{11}NiO_{40}H$	0.36	12
RefA	$(NH_4)_6H_2W_{12}O_{40} + Ni(NO_3)_2$	0.125	12
RefB	$(NH_4)_6H_2W_{12}O_{40} + Ni(NO_3)_2$	0.17	12
RefC	$(NH_4)_6H_2W_{12}O_{40} + Ni(NO_3)_2$	0.36	12

2.5. Catalytic testing

Toluene hydrogenation test was conducted at 623 K and 6 MPa. The liquid feed contained 73.6 wt% cyclohexane (used as solvent), 20.0 wt% toluene, 5.9 wt% dimethyldisulfide, used as sulfiding agent and 0.5 wt% aniline. Aniline was present to inhibit the acid function in order to avoid isomerisation reactions. This test was proceeded to evaluate and to compare the hydrogenation function of each prepared catalyst. The H_2/feed ratio was constant and equal to 450 Nl/l. The liquid feed flow was 16 $cm^3\,h^{-1}$ (LHSV of 4 h^{-1}) during the sulfidation stage and 8 $cm^3\,h^{-1}$ (LHSV of 2 h^{-1}) during the catalytic test. Catalyst balls were filtered and their diameter did not exceed 3 mm. This fraction was diluted in solid SiC (4 cm^3 for 4 cm^3 of catalyst). After sulfidation (2 °C min^{-1} followed by 2 h at 350 °C), conversions were determined by the analysis of effluent through on-line gas chromatography every 45 min after the first measurement. Catalytic results were expressed in terms of toluene hydrogenation (HYD) reaction rates, calculated from the measured toluene conversions (hydrogenation products).

3. Results and discussion

The experimental Ni/W ratios reported in Table 1 were in agreement with those expected from the preparation. Fig. 2 showed the Raman spectra of nickel salts $Ni_{3/2}PW_{12}O_{40}$, $Ni_2SiW_{12}O_{40}$, $Ni_3PW_{11}NiO_{40}H$ and of $(NH_4)_4NiW_6O_{24}H_6$. In this figure are also reported Raman spectra of the starting materials $H_3PW_{12}O_{40}$ and $H_4SiW_{12}O_{40}$ whose lines characteristic of the W–O terminal stretching mode are observed at 1011 and 998 cm^{-1} respectively, in agreement with literature data [8,9]. Raman spectra of the nickel salts indicated that the Keggin structures $PW_{12}O_{40}^{3-}$ and $SiW_{12}O_{40}^{4-}$ were preserved after the ionic exchange by comparison with spectra of the corresponding heteropolyacids. ^{31}P NMR (spectra not reported here) analysis confirmed this result with the chemical shift observed at −15.4 ppm for $Ni_{3/2}PW_{12}O_{40}$ in agreement with values already reported for the $PW_{12}O_{40}^{3-}$ Keggin entities [10]. In Fig. 2-f corresponding to $NiW_6O_{24}H_6^{4-}$ ammonium salt, the main line corresponding to W–O terminal vibration mode is observed at 947 cm^{-1}; this feature and the whole spectrum (not presented here) are characteristic of Anderson HPA structure (Tungsten or Molybdenum based) as already observed for $Al(Co)Mo_6O_{24}H_6^{3-}$ [11]. The nickel salt of $PW_{11}NiO_{40}H^{6-}$ did not exhibit the same line as observed for $Ni_{3/2}PW_{12}O_{40}$ but presented a characteristic line at 989 cm^{-1} corresponding to the W–O terminal vibration mode of the HPA. In the preparation procedure (Fig. 1), when pH was raised with the addition of 3.5 equivalent of barium hydroxide, the Keggin anion which is kinetically stable only at pH < 3, was then converted into the so-called lacunary anion. In Fig. 2-d a slight extra-peak at 988 cm^{-1} is observed indicating probably the presence of some lacunary species $SiW_{11}O_{39}^{8-}$. Their formation could be explained by the preparation procedure and local pH increase in the solution during barium hydroxide addition.

IR analyses allowed us to follow the preparation procedure associated to $Ni_3PW_{11}NiO_{40}H$. In Fig. 3 are reported the IR spectra of the barium and nickel salts of the lacunary HPA and the nickel salts of $PW_{12}O_{40}^{3-}$ and $SiW_{12}O_{40}^{4-}$. Typical absorption bands of such anions were observed in the range 500–1100 cm^{-1} [8]. The spectrum of the $Ba_{7/2}PW_{11}O_{39}$ salt (Fig. 3-c) shows two bands at 1089 and 1044 cm^{-1} assigned to the vibration ν P–O of the central PO_4 tetrahedron. In fact, the prominent band observed at 1080 cm^{-1} (Fig. 3-b) for the ν P–O vibration in Keggin HPA $PW_{12}O_{40}^{3-}$ splits into two components due to the symmetry decrease of the PO_4 tetrahedron in $PW_{11}O_{39}^{7-}$. In the IR spectrum of the corresponding nickel salt, the observation of one band at 1062 cm^{-1} clearly indicates that Ni cations restore the symmetry of the central tetrahedron and are inserted in the HPA structure to form the $PW_{11}NiO_{40}H^{6-}$ anion [12]. FT-IR spectrum 3-a (Fig. 3-a) is characteristic of $SiW_{12}O_{40}^{4-}$ HPA in agreement with literature data [8], showing again that this HPA is not modified during ionic exchange to form its nickel salt.

The aqueous solutions of the nickel salts $Ni_{3/2}PW_{12}O_{40}$, $Ni_2SiW_{12}O_{40}$, $Ni_3PW_{11}NiO_{40}H$ have been used to prepare ASA supported catalysts. Characterization of the catalysts at each step of the preparation

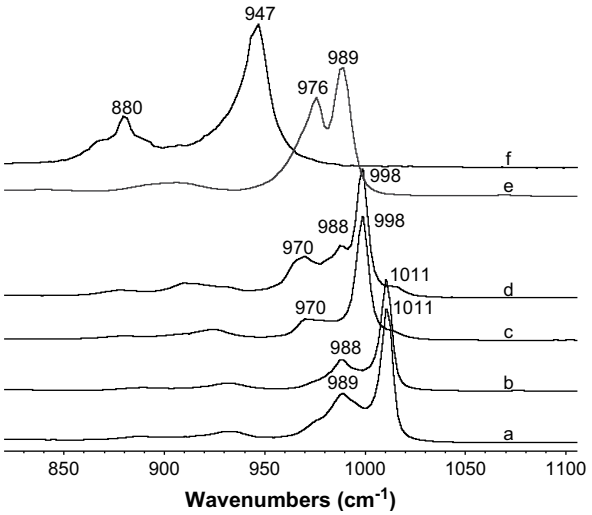

Fig. 2. Raman spectra of $H_3PW_{12}O_{40}$ (a) $Ni_{3/2}PW_{12}O_{40}$ (b) $H_4SiW_{12}O_{40}$ (c) $Ni_2SiW_{12}O_{40}$ (d) $Ni_3PW_{11}NiO_{40}H$ (e) and $(NH_4)_4NiW_6O_{24}H_6$ (f).

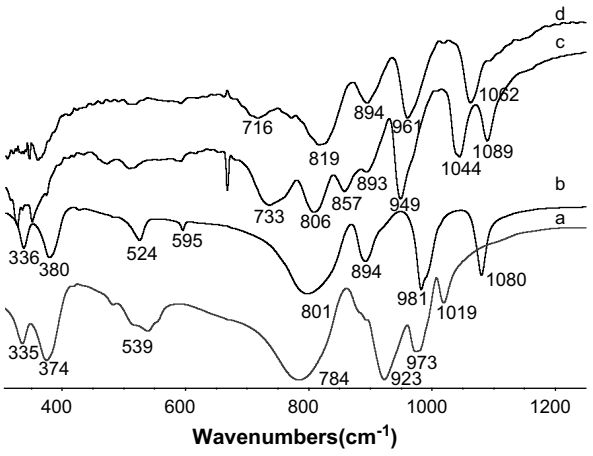

Fig. 3. IR spectra of $Ni_2SiW_{12}O_{40}$ (a) $Ni_{3/2}PW_{12}O_{40}$ (b) $Ba_{7/2}PW_{11}O_{39}$ (c) and $Ni_3PW_{11}NiO_{40}H$ (d).

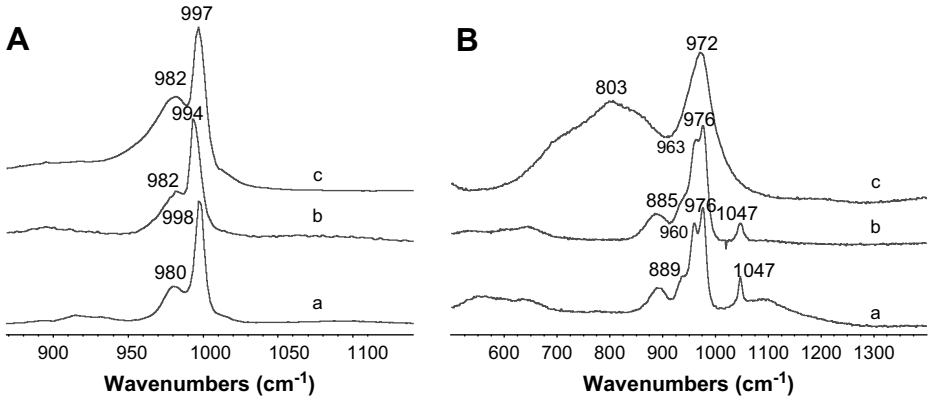

Fig. 4. Raman spectra of $Ni_2SiW_{12}O_{40}$ (A) impregnating solution (A,a), B catalyst after drying (A,b), B catalyst after calcination (A,c), and of conventional catalyst (B) impregnating solution (B,a), ref B catalyst after drying (B,b) and ref B catalyst after calcination (B,c).

by Raman spectroscopy allowed us to follow the evolution of the starting materials upon drying and calcination (Figs. 4 and 5). A catalyst prepared from conventional starting materials ammonium metatungstate and nickel nitrate was also studied for comparison purposes.

The Raman spectra of the conventional (Fig. 4-B,b), $Ni_2SiW_{12}O_{40}$ (Fig. 4-A,b) and $Ni_3PW_{11}NiO_{40}H$ (Fig. 5-B,a) dried catalysts present almost the same lines as the starting material (Figs. 4-B,a, A,a and 5-B,a). Only weak broadening and shift due to support effect were observed indicating HPA entities preservation on the ASA support after drying. However $Ni_{3/2}PW_{12}O_{40}$ features (Fig. 5-A,a) are not clearly observed in the corresponding dried catalyst (Fig. 5-A,b). After calcination, the large band around 967–972 cm^{-1} is attributed to the formation of a well-dispersed polytungstate phase for $Ni_3PW_{11}NiO_{40}H$, $Ni_{3/2}PW_{12}O_{40}$ (Fig. 5-A,c, B,c) and the conventional catalyst (Fig. 4-B,c). Raman spectrum of $Ni_2SiW_{12}O_{40}$ calcined catalyst is rather different and one can observe the $SiW_{12}O_{40}^{4-}$ HPA features. $SiW_{12}O_{40}^{4-}$ entities which are destroyed during calcination at 500 °C are certainly re-formed after thermal treatment and transfer in air.

The toluene hydrogenation test was performed on catalysts described in Table 1. Results are reported in Fig. 6 and demonstrate that A, B and C catalysts were active in toluene hydrogenation. As observed for conventional catalysts, the activity of the HPA based catalyst increased when the Ni/W ratio was raised. Moreover, HPA based catalysts which contain phosphorus are slightly more efficient as the reference ones.

Transmission electron microscopy (TEM) was used to evaluate the morphology of the WS_2 crystallites obtained after sulfidation. Taking into account the catalytic results, we focused this study on $Ni_{3/2}PW_{12}O_{40}$ and $Ni_3PW_{11}NiO_{40}H$ catalysts and the corresponding conventional catalysts with Ni/W = 0.125 and Ni/W = 0.36. As already mentioned in the literature [13] one can observe an inhomogeneous distribution of the WS_2 slabs on ASA support. A typical TEM micrograph is shown in Fig. 7 that corresponds to

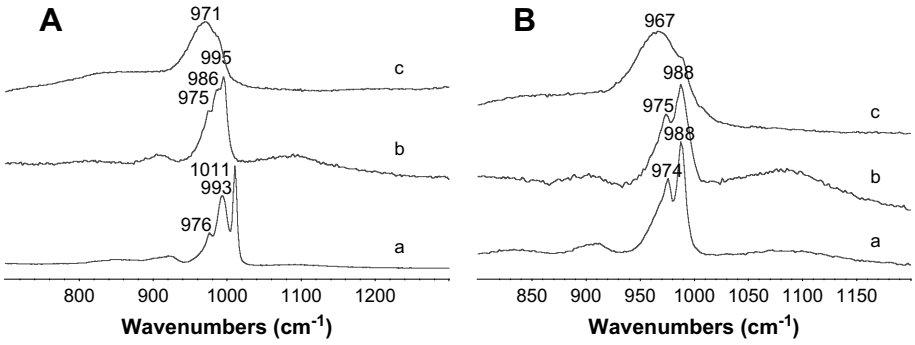

Fig. 5. Raman spectra of $Ni_{3/2}PW_{12}O_{40}$ (A) impregnating solution (A,a), A catalyst after drying (A,b), A catalyst after calcination (A,c), and of $Ni_3PW_{11}NiO_{40}H$ (B) impregnating solution (B,a), C catalyst after drying (B,b) and C catalyst after calcination (B,c).

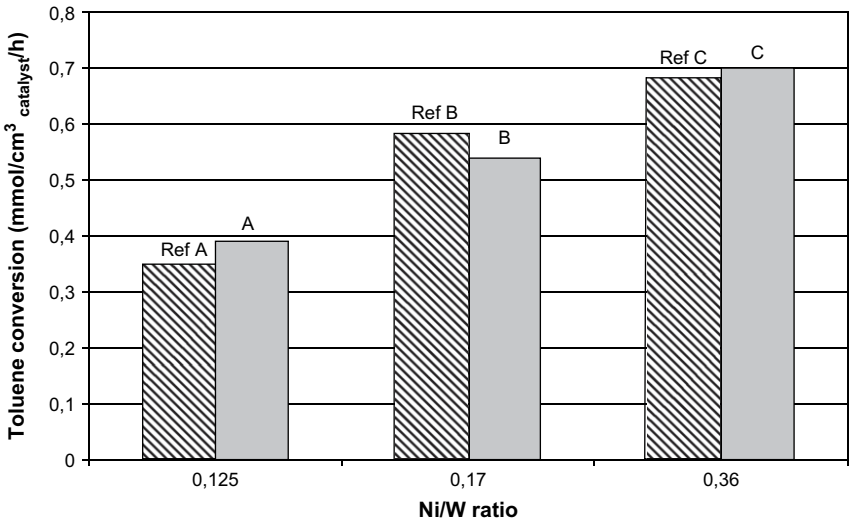

Fig. 6. Hydrogenation activity of catalysts prepared with conventional impregnating solutions (hatched) and HPA nickel salts (bicolore).

$Ni_3PW_{11}NiO_{40}H$ catalyst. The average slab lengths and stacking degrees of catalysts are listed in Table 2. These results show that the average length and stacking of the HPA based catalysts were higher than those obtained for the conventional ones. However, whatever the material is, the average length (between 14.6 and 20.8 Å) is smaller than values reported for WS_2 on ASA support [13] and for MoS_2 supported phase [14]. As shown in Fig. 8 for $Ni_3PW_{11}NiO_{40}H$ catalyst whose slabs are the largest for this study, the majority of the slabs have a length between 10 and 20 Å. This is also observed for reference catalyst C.

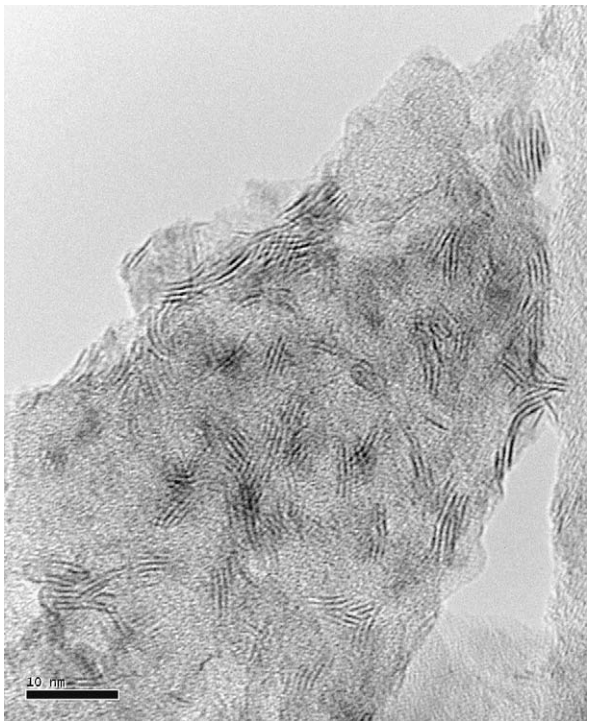

Fig. 7. TEM picture of $Ni_3PW_{11}NiO_{40}H$ catalyst.

The dispersion of the WS_2 crystallites seems to be better in conventional catalysts and does not explain the catalytic results. As it was already reported for CoMo catalyst [15,16], the efficiency of HPA catalyst could arise from the promoting effect that is enhanced by the proximity of Ni and W in HPA nickel salt used in the impregnating solution.

4. Conclusion

In this work, well-characterized heteropolytungstate nickel salts were used to prepare supported ASA hydrocracking catalysts. Each step of catalyst preparation was followed by Raman analysis: in most catalysts, HPA are preserved after drying and a well-dispersed polytungstate phase is present after calcination except for $Ni_2SiW_{12}O_{40}$ where $SiW_{12}O_{40}^{4-}$ HPA could re-form after calcination and

Table 2
Average slab length, average stacking degree of studied catalysts.

Catalysts nomenclature	Average slab length (Å)	Average stacking degree
A	17.3	1.23
RefA	14.6	1.19
C	20.8	1.53
RefC	17.9	1.49

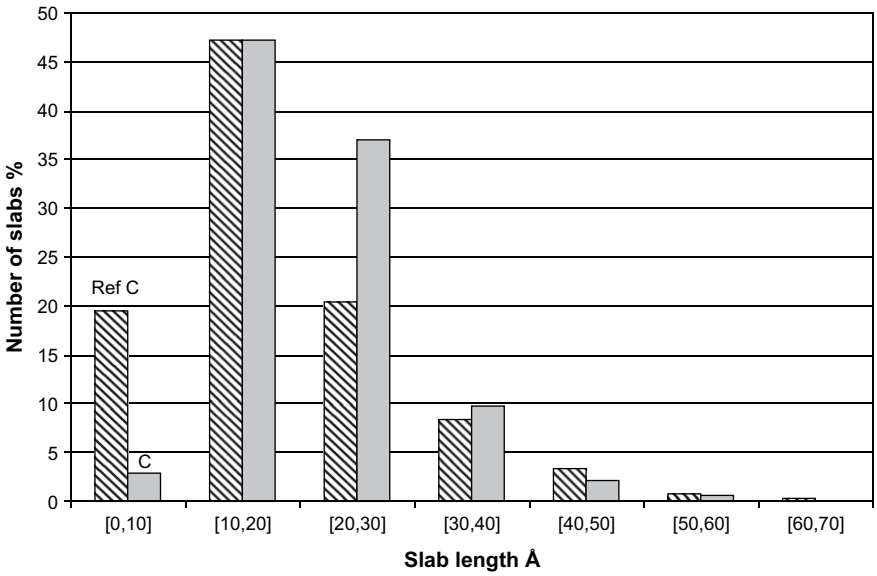

Fig. 8. Slab length distribution of $Ni_3PW_{11}NiO_{40}H$ catalyst (bicolore) and its corresponding conventional catalyst (hatched).

transfer in air. Hydrogenation activity of HPA based catalysts was also compared to conventional preparation. Results showed that new starting materials based catalysts were almost equivalent to their reference prepared by using the conventional impregnating solutions of ammonium metatungstate and nickel nitrate. A slight increase is observed by using $Ni_{3/2}PW_{12}O_{40}$ and $Ni_3PW_{11}NiO_{40}H$ catalysts. TEM results showed that WS_2 dispersion in conventional catalysts was higher than the dispersion observed in HPA catalysts. In these catalysts, a better promoting effect could explain the catalytic results. It could be due to the use of the HPA nickel salt which allows a proximity between W and Ni.

Nevertheless, further characterizations of the sulfided solids are under progress to better understand the influence of the use of these new HPA starting materials on their catalytic behavior.

References

[1] K. Sato, Y. Iwata, Y. Miki, H. Shimada, J. Catal. 186 (1999) 45.
[2] A.M. Alsobaai, R. Zakaria, B.H. Hameed, Chem. Eng. J. 132 (2007) 173.
[3] M. Roussel, J.L. Lemberton, M. Guisnet, T. Cseri, E. Benazzi, J. Catal. 218 (2003) 427.
[4] M. Roussel, S. Norsic, J.L. Lemberton, M. Guisnet, T. Cseri, E. Benazzi, Appl. Catal. A 279 (2005) 53.
[5] E. Matijevic, M. Kerker, H. Beyer, F. Theubert, Inorg. Chem. 3 (1963) 581.
[6] P. Souchay, Ions minéraux condensés, Masson et Cie, 1969, pp. 92.
[7] E.O. North, Inorg. Synth. 1 (1939) 129.
[8] C. Rocchiccioli-Deltcheff, M. Fournier, R. Franck, R. Thouvenot, Inorg. Chem. 22 (1983) 207.
[9] C. Rocchiccioli-Deltcheff, R. Thouvenot, R. Franck, Spectrochim. Acta A32 (1976) 587.
[10] R. Massart, R. Contant, J.M. Fruchart, J.P. Ciabrini, M. Fournier, Inorg. Chem. 16 (11) (1977) 2916.
[11] C. Martin, C. Lamonier, M. Fournier, O. Mentré, V. Harlé, D. Guillaume, E. Payen, Inorg. Chem. 43 (15) (2004) 4636.
[12] L.R. Pizzio, M.N. Blanco, Mat. Lett. 61 (2007) 719.
[13] Y. van der Meer, E.J.M. Hensen, J.A.R. van Veen, A.M. van der Kraan, J. Catal. 228 (2004) 433.
[14] J. Mazurelle, C. Lamonier, C. Lancelot, E. Payen, C. Pichon, D. Guillaume, Catal. Today 130 (2008) 41.
[15] C. Martin, C. Lamonier, M. Fournier, O. Mentré, V. Harlé, D. Guillaume, E. Payen, Chem. Mater. 17 (2005) 4438.
[16] C. Lamonier, C. Martin, J. Mazurelle, V. Harlé, D. Guillaume, E. Payen, Appl. Catal. B: Env. 70 (2007) 548.